5-[4-(Diethoxyphosphoryl)-2,3,5,6-tetrafluorophenyl]-10,15,20-tris-(pentafluorophenyl)porphyrin

Carla F. Pereira,[a,b] José A. Fernandes,[b] João M. M. Rodrigues,[c] Sérgio M. F. Vilela,[b] João P. C. Tomé[c] and Filipe A. Almeida Paz[b]*

[a]Department of Chemistry, University of Aveiro, QOPNA, 3810-193 Aveiro, Portugal, [b]Department of Chemistry, University of Aveiro, CICECO, 3810-193 Aveiro, Portugal, and [c]Department of Chemistry, University of Aveiro, QOPNA, 3810-193 Aveiro, Portugal
Correspondence e-mail: filipe.paz@ua.pt

The title compound, $C_{48}H_{20}F_{19}N_4O_3P$, prepared by the nucleophilic attack of triethyl phosphite on one of the 4-fluoro atoms of 5,10,15,20-tetrakis(pentafluorophenyl)porphyrin, contains a single molecule in the asymmetric unit. The porphyrin unit is almost planar [largest non-H atom deviation = 0.174 (6) Å], and has the planes of the neighbouring benzene rings oriented at angles ranging from 64.3 (2) to 89.6 (3)° relative to the porphyrin core. The P=O group is almost coplanar with the attached benzene ring, subtending an angle of 4.0 (3)°. Several weak supramolecular interactions, namely C—H···π, C—F···π, P=O···π, C—H···(O,F) and F···F contacts, contribute to the crystal packing.

Comment

New synthetic strategies and primary building blocks have been developed for the specific design of multidimensional coordination polymers which combine a wide range of metallic centres with ligands having multiple binding sites. For this purpose, porphyrin macrocycles can be designed having several coordination-capable groups located at the periphery of their core, which may ultimately also allow fine tuning of the framework topology (Natarajan & Mahata, 2009; Choi et al., 2009). Compared with carboxylate-based ligands, phosphonates are less commonly used to prepare coordination polymers, due to three main factors: (i) dense layered materials are usually formed, compared with the more interesting porous frameworks which may exhibit high surface areas; (ii) the growth of single crystals with phosphonates is generally more difficult because they often precipitate rapidly as less ordered and insoluble phases; (iii) the coordination chemistry of phosphonate groups is more complex due to their various stages of deprotonation (Natarajan & Mahata, 2009; Shimizu et al., 2009). Despite all these limitations, phosphonate-based ligands are still highly attractive molecules to prepare hybrid materials with different structures and interesting properties.

A search of the literature yields only a handful of phosphorylporphyrins (Atefi et al., 2006; Enakieva et al., 2009; Matano et al., 2007), which may be employed as precursor structural building blocks for multiporphyrin arrays and networks (Natarajan & Mahata, 2009; Shimizu et al., 2009). Following our research interest in the use of phosphonate-based organic ligands for the construction of coordination polymers (Cunha-Silva, Lima et al., 2009; Cunha-Silva, Ananias et al., 2009; Cunha-Silva et al., 2007; Shi et al., 2008; Silva et al., 2011), we report herein the synthesis, structural characterization and crystallographic details of an isolated intermediate molecule, namely 5-[4-(diethoxyphosphoryl)-2,3,5,6-tetrafluorophenyl]-10,15,20-tris(pentafluorophenyl)-porphyrin, (I), obtained in our quest to isolate phosphonic acid-based porphyrin molecules for self-assembly with metallic centres.

(I)
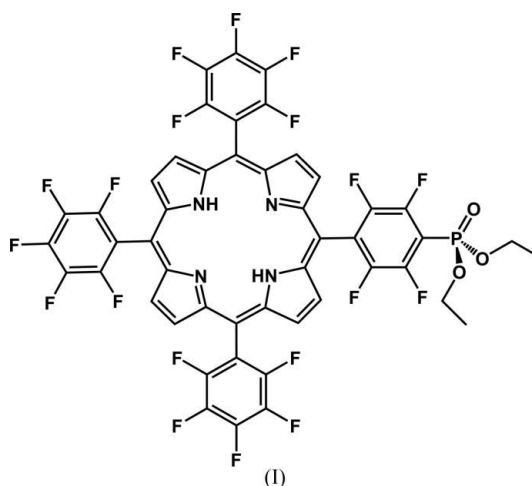
The asymmetric unit of (I) comprises a single molecule of the porphyrin derivative (Fig. 1). The porphyrin central core is approximately planar, with the largest distance from one atom (C14) to the average plane being 0.174 (6) Å. The substituent benzene rings subtend angles with the porphyrin core in the range 64.3 (2)–89.6 (3)°. These values agree well with those typically observed in related materials [a search of the Cambridge Structural Database (Version 5.32; Allen, 2002) yields 66 hits, with all of the angles being in the range ca 60–90°, with a mean of 77.5°], and allow a minimization of the steric repulsion between the F atoms and the porphyrin core.

The P=O group of the phosphoryl moiety is located in the approximate average plane of the benzene ring to which it is attached [the ring···P=O angle is about 4.0 (3)°]. This conformation of the phosphoryl group enables a significant reduction of the steric impediment associated with the presence of the two pendant and highly flexible ethyl groups (Fig. 1). The conformational arrangements of the two ethyl substituents are different. Firstly, while methylene atom C1 forms an antiperiplanar angle with its neighbouring O3—P1—C28 group, for methylene atom C3 the antiperiplanar angle is instead formed with its neighbouring O2—P1—O3 group.
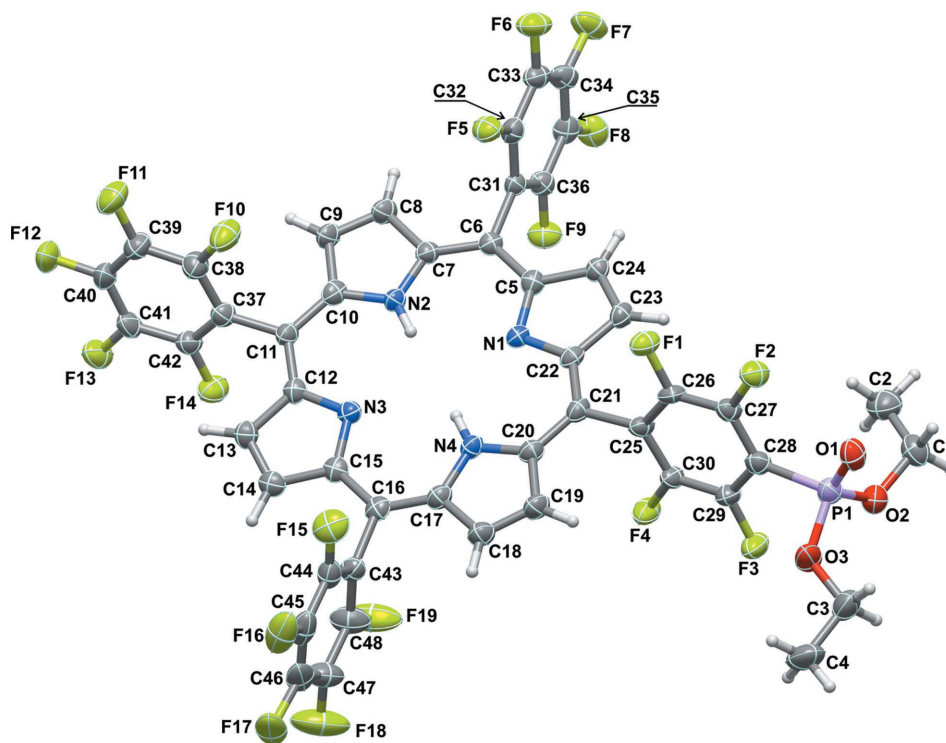
Figure 1
The molecular structure of (I), showing the atom-labelling scheme. Displacement ellipsoids are drawn at the 50% probability level.

Secondly, the two torsion angles involving the terminal methyl groups are also not similar, being (−)-synclinal for P1—O2—C1—C2 and (+)-antiperiplanar for P1—O3—C3—C4 (Table 1).

The molecule of (I) lacks typical hydrogen-bonding donors, and therefore strong supramolecular interactions mediating the crystal packing are absent. In addition, the asymmetric nature of the molecule also seems to avoid the presence of
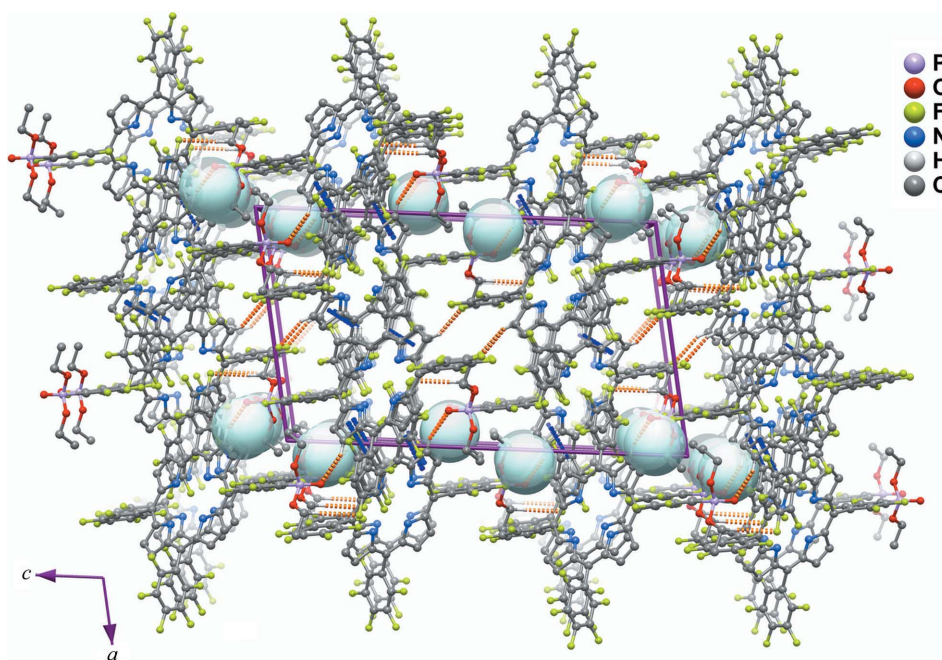

Figure 2
A schematic representation of the crystal packing of (I), viewed in perspective along the [0$\bar{1}$0] direction of the unit cell. H atoms not engaged in supramolecular interactions (dashed lines) have been omitted for clarity [in the electronic version of the paper, C—H···(N,O) interactions are orange dashed lines and C—H···π interactions are blue dashed lines]. The void volumes within the crystal structure are depicted schematically as transparent (blue) spheres.

typical π–π interactions. Thus, the crystal packing is ensured by weak interactions such as C—H$\cdots\pi$, C—F$\cdots\pi$, P=O$\cdots\pi$, C—H$\cdots$(O,F) and F$\cdots$F contacts (Fig. 2; see Table 2 for geometric details of all these interactions). Molecules of (I) form supramolecular layers in the *ab* plane of the unit cell, having essentially C—H$\cdots\pi$ contacts between the cores of adjacent porphyrin rings. The bulky phosphonate groups point towards these interlayer spaces and are engaged in a number of weak C—H$\cdots$O and C—H$\cdots$F interactions (Fig. 2 and Table 2).

It is noteworthy that the crystal structure contains a small void volume of *ca* 46 Å^3 (Fig. 2). Although this empty space is suitable for the inclusion of a small solvent molecule, such as water, the total electron density found within the cavity is less than four electrons and highly smeared out, thus avoiding a sensible location and refinement of additional molecular entities within the crystal structure.

Experimental

Chemicals and solvents were purchased from commercial sources and used as received. 5,10,15,20-Tetrakis(pentafluorophenyl)porphyrin (TPPF$_{20}$) was prepared according to a published procedure (Tomé *et al.*, 2005). To a solution of TPPF$_{20}$ (25 mg, 25.7 µmol) in dry toluene (2.5 ml; Riedel-de-Haën, 99,7%), triethyl phosphite was added in excess (1.0 ml, 5.8 mmol; Sigma–Aldrich, 98%) and the mixture was stirred under reflux for 48 h under a nitrogen atmosphere. Toluene and the excess of triethyl phosphite were distilled off under reduced pressure. The crude mixture was purified by column chromatography using dichloromethane as eluent. Compound (I) was recrystallized from a mixture of dichloromethane and methanol (1:3 *v/v*) at ambient temperature (yield 22%). ^{1}H NMR (300 MHz, CDCl$_3$): δ 8.93 (*d*, *J* = 3.3 Hz, 8H, β-H), 4.66–4.44 (*m*, 4H, CH$_2$), 1.59 (*t*, *J* = 7.0 Hz, 6H, CH$_3$), −2.92 (*s*, 2H, NH); ^{19}F NMR (282 MHz, CDCl$_3$): δ −155.26 (*dd*, *J* = 23.7 and 13.6 Hz, 2F, 5-Ar-*o*-F), −158.79 to −159.02 (*m*, 2F, 5-Ar-*m*-F), −160.02 (*dd*, *J* = 24.3 and 7.4 Hz, 6F, 10,15,20-Ar-*o*-F), −174.70 (*t*, *J* = 20.9 Hz, 3F, 10,15,20-Ar-*p*-F), −184.63 to −184.96 (*m*, 6F, 10,15,20-Ar-*m*-F); ^{31}P NMR (121 MHz, CDCl$_3$): δ 5.80 (*s*, *R*–PO$_3$Et$_2$).

Crystal data

C$_{48}$H$_{20}$F$_{19}$N$_4$O$_3$P	V = 4539.3 (11) Å^3
M_r = 1092.65	Z = 4
Monoclinic, $P2_1/c$	Mo $K\alpha$ radiation
a = 15.530 (2) Å	μ = 0.19 mm^{-1}
b = 11.2539 (17) Å	T = 150 K
c = 26.375 (3) Å	0.08 × 0.05 × 0.03 mm
β = 100.024 (9)°	

Data collection

Bruker APEXII X8 KappaCCD area-detector diffractometer	32626 measured reflections
	8275 independent reflections
Absorption correction: multi-scan (*SADABS*; Sheldrick, 1997)	3504 reflections with $I > 2\sigma(I)$
T_{min} = 0.985, T_{max} = 0.994	R_{int} = 0.115

Refinement

$R[F^2 > 2\sigma(F^2)]$ = 0.084	678 parameters
$wR(F^2)$ = 0.271	H-atom parameters constrained
S = 0.99	$\Delta\rho_{max}$ = 0.42 e Å^{-3}
8275 reflections	$\Delta\rho_{min}$ = −0.34 e Å^{-3}

Table 1
Selected torsion angles (°).

O3—P1—O2—C1	−167.3 (4)	P1—O2—C1—C2	−81.5 (7)
C28—P1—O3—C3	178.3 (6)	P1—O3—C3—C4	166.7 (6)

Table 2
Selected supramolecular interactions (Å, °).

*Cg*1, *Cg*2, *Cg*3 and *Cg*4 are the centroids of the rings N1/C5/C22–C24, N3/C12–C15, N2/C7–C10 and C31–C36, respectively.

C—H$\cdots A$	C—H	H$\cdots A$	C$\cdots A$	C—H$\cdots A$
C3—H3*A*$\cdots$F7^{iii}	0.99	2.52	3.487 (9)	167
C13—H13$\cdots$F12^{iv}	0.95	2.42	3.062 (7)	124
C24—H24$\cdots$O1^{iii}	0.95	2.43	3.327 (7)	157

C—F$\cdots$F—C	C—F/F—C	F$\cdots$F	C—F$\cdots$F	F$\cdots$F—C
C35—F8$\cdots$(F15—C44)^v	1.360 (7)/ 1.320 (8)	2.887 (6)	164.6 (4)	133.9 (4)
C39—F11$\cdots$(F19—C48)^{vi}	1.353 (8)/ 1.324 (8)	2.763 (7)	121.6 (4)	165.8 (4)

C—H$\cdots Cg$	C—H	H$\cdots Cg$	C$\cdots Cg$	C—H$\cdots Cg$
C8—H8$\cdots$*Cg*1^i	0.95	2.96	3.842 (7)	155
C18—H18$\cdots$*Cg*2^{ii}	0.95	2.83	3.552 (7)	133

C—F$\cdots Cg$	C—F	F$\cdots Cg$	C$\cdots Cg$	C—F$\cdots Cg$
C33—F6$\cdots$*Cg*3^i	1.337 (7)	3.576 (5)	4.454 (7)	123.4 (3)
C46—F17$\cdots$*Cg*1^{ii}	1.358 (8)	3.124 (6)	4.157 (11)	131.9 (5)

P=O$\cdots Cg$	P=O	O$\cdots Cg$	P$\cdots Cg$	P=O$\cdots Cg$
P1—O1$\cdots$*Cg*4^{iii}	1.444 (5)	3.372 (5)	4.395 (3)	127.0 (2)

Symmetry codes: (i) $-x, y + \frac{1}{2}, -z + \frac{3}{2}$; (ii) $-x + 1, y - \frac{1}{2}, -z + \frac{3}{2}$; (iii) $-x, -y, -z + 1$; (iv) $-x + 1, -y + 1, -z + 2$; (v) $x - 1, y, z$; (vi) $x, y + 1, z$.

H atoms bound to C and N atoms were placed at their idealized positions and included in the final structural model in the riding-motion approximation, with C—H = 0.95 (aromatic), 0.99 (methylene) or 0.98 Å (methyl) and N—H = 0.88 Å. The isotropic displacement parameters for these atoms were fixed at 1.5U_{eq}(C) for methyl H atoms and 1.2U_{eq}(parent) otherwise.

Crystals of (I) were systematically isolated as very small blocks. The largest crystal isolated from several batches had a maximum dimension of 0.08 mm and, even for long exposure times at 150 K, the R_{int} value for a resolution better than *ca* 1.2 Å was always above 0.10. At this resolution range, in particular between 0.99 and 0.96 Å, the crystal diffracted very weakly, with the mean I/σ value being only of about 1.3. In addition, the existence of empty voids within the crystal structure, which most certainly contain highly disordered solvent molecules, also contributed to the high refined R factors.

Data collection: *APEX2* (Bruker, 2006); cell refinement: *APEX2*; data reduction: *SAINT-Plus* (Bruker, 2005); program(s) used to solve structure: *SHELXTL* (Sheldrick, 2008); program(s) used to refine structure: *SHELXTL*; molecular graphics: *DIAMOND* (Brandenburg, 2009); software used to prepare material for publication: *SHELXTL*.

References

Allen, F. H. (2002). *Acta Cryst.* B**58**, 380–388.

Atefi, F., McMurtrie, J. C., Duriska, M. & Arnold, D. P. (2006). *Inorg. Chem.* **45**, 6479–6489.

Brandenburg, K. (2009). *DIAMOND*. Crystal Impact GbR, Bonn, Germany.

Bruker (2005). *SAINT-Plus*. Bruker AXS Inc., Madison, Wisconsin, USA.

Bruker (2006). *APEX2*. Bruker AXS Inc., Madison, Wisconsin, USA.

Choi, E.-Y., Barron, P. M., Novotny, R. W., Son, H.-T., Hu, C. & Choe, W. (2009). *Inorg. Chem.* **48**, 426–428.

Cunha-Silva, L., Ananias, D., Carlos, L. D., Paz, F. A. A. & Rocha, J. (2009). *Z. Kristallogr.* **224**, 261–272.

Cunha-Silva, L., Lima, S., Ananias, D., Silva, P., Mafra, L., Carlos, L. D., Pillinger, M., Valente, A. A., Paz, F. A. A. & Rocha, J. (2009). *J. Mater. Chem.* **19**, 2618–2632.

Cunha-Silva, L., Mafra, L., Ananias, D., Carlos, L. D., Rocha, J. & Paz, F. A. A. (2007). *Chem. Mater.* **19**, 3527–3538.

Enakieva, Y. Y., Bessmertnykh, A. G., Gorbunova, Y. G., Stern, C., Rousselin, Y., Tsivadze, A. Y. & Guilard, R. (2009). *Org. Lett.* **11**, 3842–3845.

Matano, Y., Matsumoto, K., Terasaka, Y., Hotta, H., Araki, Y., Ito, O., Shiro, M., Sasamori, T., Tokitoh, N. & Imahori, H. (2007). *Chem. Eur. J.* **13**, 891–901.

Natarajan, S. & Mahata, P. (2009). *Curr. Opin. Solid State Mater. Sci.* **13**, 46–53.

Sheldrick, G. M. (1997). *SADABS*. Bruker AXS Inc., Madison, Wisconsin, USA.

Sheldrick, G. M. (2008). *Acta Cryst.* A**64**, 112–122.

Shi, F.-N., Cunha-Silva, L., Ferreira, R. A. S., Mafra, L., Trindade, T., Carlos, L. D., Paz, F. A. A. & Rocha, J. (2008). *J. Am. Chem. Soc.* **130**, 150–167.

Shimizu, G. K. H., Vaidhyanathan, R. & Taylor, J. M. (2009). *Chem. Soc. Rev.* **38**, 1430–1449.

Silva, P., Vieira, F., Gomes, A. C., Ananias, D., Fernandes, J. A., Bruno, S. M., Soares, R., Valente, A. A., Rocha, J. & Paz, F. A. A. (2011). *J. Am. Chem. Soc.* **133**, 15120–15138.

Tomé, J. P. C., Neves, M. G. P. M. S., Tomé, A. C., Cavaleiro, J. A. S., Mendonça, A. F., Pegado, I. N., Duarte, R. R. & Valdeira, M. L. (2005). *Bioorg. Med. Chem.* **13**, 3878–3888.